

Anaplastic Transformation in Myxopapillary Ependymoma: A Report of 2 Cases and Review of the Literature

Lorenzo Gitto, MD, Serenella Serinelli, MD, Kristyn Galbraith, MD, Michael Williams, MD, Kanish Mirchia, MD, Michael A. Galgano, MD, Satish Krishnamurthy, MD, Gustavo de la Roza, MD, Mariano S. Viapiano, PhD, Jamie M. Walker, MD, PhD, George Jour, MD, Jonathan Serrano, BS, Michael DeLorenzo, BS, Matija Snuderl, MD, and Timothy E. Richardson, DO, PhD

Abstract

Myxopapillary ependymoma (MPE) is a relatively common neoplasm arising primarily in the filum terminale/lumbosacral region of the spinal cord. It is designated as a grade I tumor in the most recent WHO Classification of Tumours of the CNS, although aggressive clinical behavior can be observed, especially in cases arising in an extradural location. Anaplastic transformation in MPE is exceedingly rare with <20 examples reported in the English literature, and consensus on diagnostic features and definitive grading remain to be determined. Here, we present 2 cases of recurrent MPE with anaplastic features, both of which had histology consistent with conventional MPE as well as areas with significant atypia, frequent mitotic figures, elevated Ki-67 proliferation indices (>10%–50%), necrosis, and focal vascular proliferation. Targeted next-generation sequencing panels revealed no definitive pathogenic mutations or fusion proteins in either case. Copy number profiling, methylation profiling, and t-Distributed Stochastic Neighbor Embedding were performed to investigate the molecular characteristics of these tumors. To the best of our knowledge, these are the first reported cases of MPE with anaplastic features with methylation profiling data. In addition, we review the literature and discuss common histologic and molecular findings associated with anaplastic features in MPE.

Key Words: Anaplasia, Anaplastic, Glioma, Myxopapillary ependymoma, Spine.

INTRODUCTION

Ependymomas are slow growing glial neoplasms that are thought to originate from the ependymal lining of the brain and spinal cord, and tend to occur in or adjacent to the ventricular system, although they may rarely occur in other locations. Ependymomas are the third most common pediatric central nervous system (CNS) tumor behind variants of astrocytoma and medulloblastoma (1), and are the most common primary tumor of the spinal cord, although they are more common in adults than children at this location (2, 3). The *World Health Organization* (WHO) classifies ependymomas into 3 grades: Grade I (myxopapillary ependymoma [MPE] and subependymoma), Grade II (conventional ependymoma), and Grade III (anaplastic ependymoma) (4).

There has been significant progress over the last several years in understanding the molecular features and tumor biology of ependymomas. According to a recent molecular classification of ependymomas by DNA methylation profiling developed by Pajyler et al (5), ependymomas arising from 3 distinct anatomic compartments (spine, posterior fossa, and supratentorial region) can be classified into 9 distinct subgroups with variable molecular profiles, age of onset, and clinical outcomes (Supplementary Data Table S1).

MPE (WHO grade I) is an ependymoma variant that preferentially occurs in the *conus medullaris/filum terminale* of the lumbosacral spinal cord (4). This entity was first reported by Kernohan in 1932 to describe a type of ependymoma characterized by mucinous changes and fibrovascular connective tissue (6). It is considered a low-grade neoplasm, and surgical excision of the tumor is usually curative when the neoplasm is completely resected, although local recurrence and spinal or brain metastases due to microscopic dissemination have been observed (7–9). This occurs more frequently in younger patients, patients with subtotal resection, and patients not treated with adjuvant radiotherapy (10). Rarely, these

From the Department of Pathology (LG, SS, KG, MW, KM, GdR, TER); Department of Neurosurgery (MAG, SK, MSV); Department of Neuroscience and Physiology (MSV), State University of New York, Upstate Medical University, Syracuse, New York; Department of Pathology and Glenn Biggs Institute for Alzheimer's & Neurodegenerative Diseases, University of Texas Health Science Center, San Antonio, Texas (JMW); Department of Pathology, New York University Langone Health, New York City, New York (GJ, JS, MD, MS).

Send correspondence to: Timothy E. Richardson, DO, PhD, Department of Pathology, State University of New York, Upstate Medical University, 750 E. Adams St., UH 6805A, Syracuse, NY 13210; E-mail: richatim@upstate.edu

Methylation profiling at NYU is supported in part by grants from the Friedberg Charitable Foundation and the Making Headway Foundation (to M.S.).

The authors have no duality or conflicts of interest to declare.

Supplementary Data can be found at academic.oup.com/jnen.

tumors can present as extradural neoplasms in the *filum terminale externa*, and in such cases tend to have more aggressive behavior with more frequent local invasion and distant spread, even in the absence of worrisome histologic features (11–20).

Typical microscopic features include cuboidal to elongated cells, radially arranged in a papillary fashion around myxoid material and hyalinized fibrovascular cores. The mitotic activity and the Ki-67 proliferation indices are generally extremely low. The presence of distant metastases from a MPE suggests malignant behavior of the tumor, and these cases may display atypical- or anaplastic-like features more frequently. Anaplastic or frankly malignant variants of MPE are exceedingly rare in the English literature, with only a handful of cases reported, even fewer cases with molecular data, and no cases that include methylation profiling data (21–26). Unlike classic ependymoma, in which histologic features of anaplasia are used clinically for grading purposes, no definitive grading criteria for anaplasia in MPE have been established, due in part to their rarity.

Herein, we present 2 patients with recurrent MPE showing anaplastic features and aggressive clinical behavior. Microscopic, immunohistochemical, and molecular studies were conducted. We describe the clinical, radiologic, pathologic, and molecular features of these 2 rare cases and provide a review of the literature.

MATERIALS AND METHODS

Case Selection and Literature Review

Two cases of recurrent MPE with anaplastic features were identified in the database of the State University of New York (SUNY) Upstate Medical Center with a search of all MPE cases with recurrence from 2000 to 2019. The following data were reviewed in each case: Clinical history, imaging results, laboratory results, operative reports, subsequent follow-up encounters, pathologic findings for each recurrence, and all available molecular data. In addition, a review of the English literature through *PubMed*, *Google Scholar*, *Cochrane*, and *Scopus* database, was performed using a combination of the following keywords: “myxopapillary,” “ependymoma,” “anaplastic,” “anaplasia,” and “malignant.”

Histology and Immunohistochemistry

Hematoxylin and eosin (H&E)-stained slides were prepared from 4- μ m-thick sections of formalin-fixed, paraffin-embedded (FFPE) tissue using standard protocols. Immunohistochemistry was performed on 4- μ m paraffin sections following heat-induced epitope retrieval using CC1 (Ventana, Tucson, AZ), then staining with GFAP (Thermo Fisher Scientific, Waltham, MA), neurofilament (Leica Biosystems, Richmond, VA), epithelial membrane antigen (EMA) (Cell Marque, Rocklin, CA), NeuN (Sigma-Aldrich, St. Louis, MO), S-100 (Thermo Fisher Scientific), CAM5.2 (Cell Marque), AE1/AE3 (Thermo Fisher Scientific), and Ki-67 (Dako, Carpinteria, CA) on either a Ventana Benchmark XT or Ventana Benchmark Ultra automated stainer, using Ventana Ultra-View Universal DAB Detection kits (Ventana, Tucson, AZs).

Methylation Studies

DNA extraction was carried out using the automated Maxwell system (Promega, Madison, WI). DNA methylation was analyzed by the Illumina EPIC Human Methylation array, assessing 850 000 CpG sites (Illumina, San Diego, CA), according to the manufacturer’s instructions at the NYU Molecular Pathology laboratory, as described previously (27). Molecular subclassification and t-Distributed Stochastic Neighbor Embedding (t-SNE) visualization was performed utilizing the cloud-based DNA methylation classifier, as described previously (28). In addition, the array data were used to calculate a low-resolution copy number profile, also previously described (29–35).

Next-Generation Sequencing

Targeted genome sequencing was performed on DNA isolated from FFPE tissue using NGS panels to evaluate 324 cancer related genes and gene rearrangements in Case 1 (Foundation Medicine, Cambridge, MA), and RNA was extracted and sequenced using a customized, clinically validated and NY State approved RNAseq panel targeting 86 cancer related genes (NYU Fusion SEQer) using Anchored Multiplex PCR (ArcherDX, Boulder, CO) in Case 2, as previously described (36).

RESULTS

Case Histories

Case 1

A 72-year-old man with a past medical history of squamous cell carcinoma of the tongue, status-post chemoradiation and brachytherapy, as well as benign prostatic hypertrophy, hypertension, obstructive sleep apnea, and depression, presented with a sacral mass found incidentally on MRI exam. A complex cystic and solid process with heterogeneous enhancement was observed behind the L5 vertebral body, the thecal sac, and spinal canal with inferior extension behind the sacrum, involving the S1 foramina. A focused pelvic and sacral MRI was performed, showing an intraspinal mass extending from the L3 through the upper S2 levels, measuring 13.0 \times 4.3 \times 2.3 cm (Fig. 1A). A needle biopsy of the mass showed a neoplasm with papillary architecture, basophilic myxoid material focally surrounding vessels, epithelioid neoplastic lining cells with bland cytology, and absent mitotic activity (Fig. 2A, B). Immunohistochemical studies demonstrated strong expression of GFAP (Fig. 2C) and S-100 (Fig. 2D) without expression of cytokeratins (CAM5.2 or AE1/AE3). The Ki-67 proliferation index was \sim 1%. A diagnosis of MPE, WHO grade I was made.

Approximately one year later, the patient began having symptoms of lower back pain radiating down the left lateral aspect of the left leg with associated numbness in his feet. A repeat MRI of the lumbar spine was performed, which showed an increase in the size of the mass with destruction of bone. The patient underwent multiple radiotherapy treatment cycles, but subsequent MRI a year later showed increased rostral extension of the tumor within the central spinal canal reaching

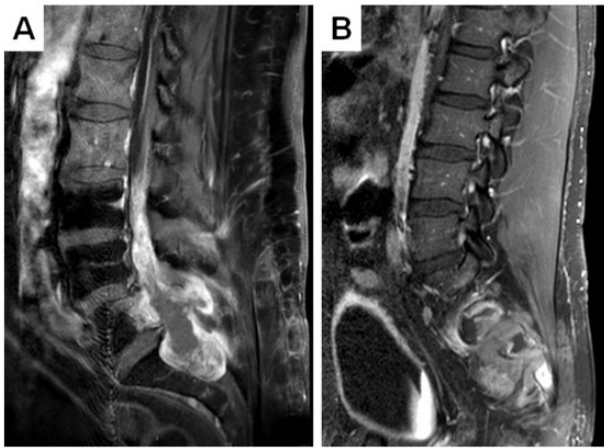


FIGURE 1. Gadolinium contrast enhancing T1 MRI images demonstrating an enhancing lesion in the lumbosacral spinal cord in patient 1 (**A**) and destruction of bone in patient 2 (**B**).

the posterior aspect of the conus at T12-L1, together with an interval increase in the size of the central necrosis of the tumor. A partial resection was performed, which showed focal retention of the classic myxopapillary architecture, including bland nuclei with myxoid material surrounding hyalinized vessels (Fig. 2E) and a more predominant area with solid tumor growth composed of large pleomorphic cells with irregular nuclei with prominent nucleoli and intranuclear inclusions, mitotic figures (8 mitoses per 10 HPF), including atypical forms (Fig. 2F), focal thickening of the vessels, and individual tumor cell necrosis. Transitional areas, characterized by more solid growth of ependymal-like cells without significant pleomorphism, were also observed between these 2 distinct histologic patterns. Immunohistochemical stains again showed strong, diffuse positivity for GFAP (Fig. 2G) and S-100 with focal areas of CAM5.2-positivity in the higher-grade areas, which were negative for AE1/AE3 and p63 antibodies, suggesting that these were part of the same tumor and not metastasis from the patient's documented squamous cell carcinoma. The Ki-67 proliferation index was now significantly elevated, above 50% (Fig. 2H). Given the transitional histology observed between the more classic MPE-like areas and the high-grade-appearing regions, as well as the similar staining pattern for GFAP and the history of biopsy-proven MPE, these changes were considered consistent with anaplastic transformation of MPE.

Adjuvant radiation treatment was performed, but the patient's condition declined after his second surgery due to a combination of medical conditions and he developed metabolic encephalopathy. He was placed on hospice care and passed away ~6 months after the last procedure.

Case 2

A 21-year-old man with a past medical history of sacral cystic mass presented with rapidly enlarging, tender mass posterior to the sacrum. A pelvic MRI demonstrated a 13.0 × 9.3 × 8.2 cm mass with internal septation abutting the sacrum and

coccyx posteriorly with possibly destruction of bone (Fig. 1B) and 2 enhancing inguinal lymph nodes, the largest of which measured 3.0 cm in the greatest dimension. A biopsy of the mass showed geographic necrosis with regions of papillary and cribriform architecture, hyalinized tissue, abundant myxoid degeneration, and scattered mitotic figures (Fig. 3A). Both the sacral neoplastic cells and lymph node metastasis were positive for GFAP (Fig. 3B), S-100, CD99, and CD56, negative for CAM5.2 (Fig. 3C), AE1/AE3, Olig2, SALL4, and OCT3/4, but focally positive for EMA (Fig. 3D). These findings were thought to be most consistent with a diagnosis of high-grade ependymoma with some histologic features suggesting malignant transformation of an MPE. The patient underwent left groin superficial inguinal lymph node dissection with resection of the primary tumor and subsequent fractionated radiation therapy. Over the following 14 months, the patient began suffering from paroxysmal suprapubic pain with numbness and weakness, and a pelvic CT scan showed worsening of the sacral ependymoma extending to the lower L5 level, with tumor filling the sacral spinal canal, destroying the adjacent bone, and compressing the lumbosacral nerves. The patient underwent an L6-S3 laminectomy with tumor resection. Microscopic examination of the tumor showed epithelioid cells with distinct cytoplasmic borders, ample eosinophilic and clear cytoplasm, and round to oval nuclei. Focal papillary architecture, myxoid material, and clearing around blood vessels, suggestive of perivascular pseudorosettes were observed. The tumor was associated with scattered foci of necrosis and tumor infiltration into the bone (Fig. 3E). Scattered mitotic figures were also present (up to 4/10 HPF). Immunohistochemical stains showed tumor cells positive for GFAP (Fig. 3F) and S-100, largely negative for EMA, and negative for CAM5.2 (Fig. 3G), with a Ki-67 proliferation index >10% (Fig. 3H). The microscopic and clinical findings were consistent with recurrent ependymoma with papillary and anaplastic features.

Methylation Analysis and t-SNE

Specimens from the recurrent tumors in both cases underwent whole-genome DNA methylation profiling and t-SNE cluster analysis (www.moleculareuropathology.org). Neither case definitively matched with any known tumor entity. Case 1 most closely matched with choroid plexus tumors (family/class score = 0.17); however, Case 2 was in closest proximity to the methylation cluster for MPE (family/class score = 0.55) (Fig. 4). *MGMT* methylation analysis revealed methylation of the *MGMT* promoter region in both cases (score = 0.55 and 0.74, respectively).

Mutation Analysis, Fusion Detection, and Copy Number Profiling

No mutations in established oncogenes or tumor suppressor genes, or pathogenic fusion proteins were identified in either case by targeted next-generation sequencing. Scattered chromosomal gains were identified in Case 1, including 3p, 4, 6, 8, 9, 12p, as well as loss on chromosome 10, 19q, 21, and 22 (Fig. 5A). Widespread chromosomal copy number changes

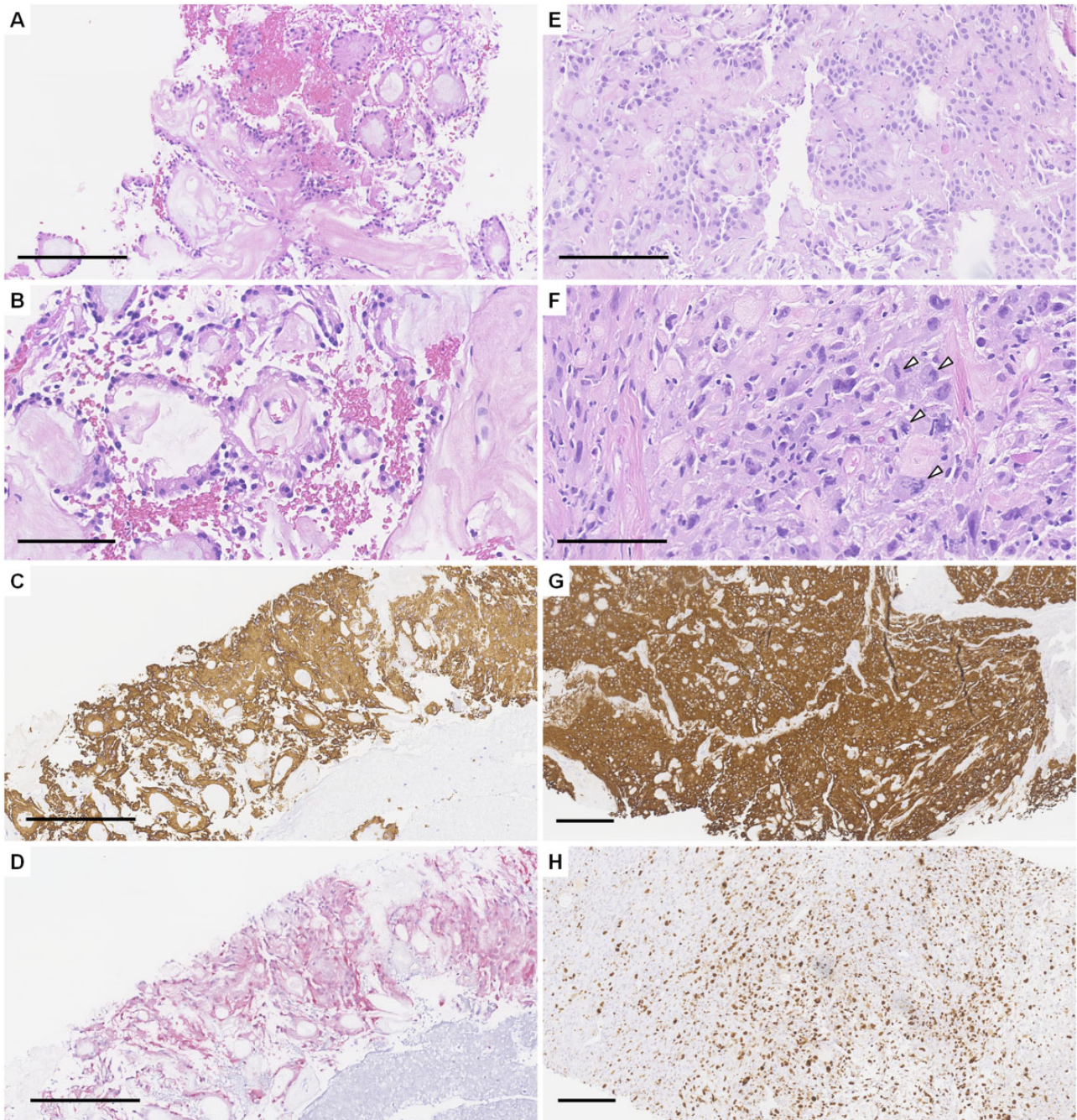


FIGURE 2. Microscopic sections from the initial biopsy of Case 1, demonstrating conventional myxopapillary ependymoma morphology on H&E staining (**A, B**), as well as strong and diffuse staining for GFAP (**C**) and S100 (**D**), as well as microscopic sections from the subsequent resection specimen showing focal retention of classic myxopapillary ependymoma histology on H&E (**E**) as well as areas of solid growth, significant atypia, and pleomorphism with frequent mitotic figures (arrowheads) (**F**). The resection specimen also demonstrated strong GFAP immunoreactivity (**G**), as well as significantly elevated Ki-67 proliferation index (**H**). Magnifications: **A, C, D, E, 200×**; **B, F, 400×**; **G, H, 100×**. Scale bars: **B, F, 100 μm**; **A, C–E, G, H, 200 μm**.

were observed in Case 2 (Fig. 5B) include relative loss of chromosomes 1, 2, 5q (focal), 6, 10, 12, 14, 17p, and 22q with relative gains in 9, 13q, and 20. This aneuploidy is similar to previous cases of MPE with anaplasia (26). Although little is known about the molecular alterations in MPE with anaplastic

change, given the paucity of reported cases in the literature, MPE frequently has gains in chromosomes 4, 5, 7, 9, 18, and 20 along with losses in chromosome 1, 2, 4, 6, and 10 (26, 37, 38). Unlike previous studies of anaplastic MPE (26), our cases demonstrated losses at 22q.

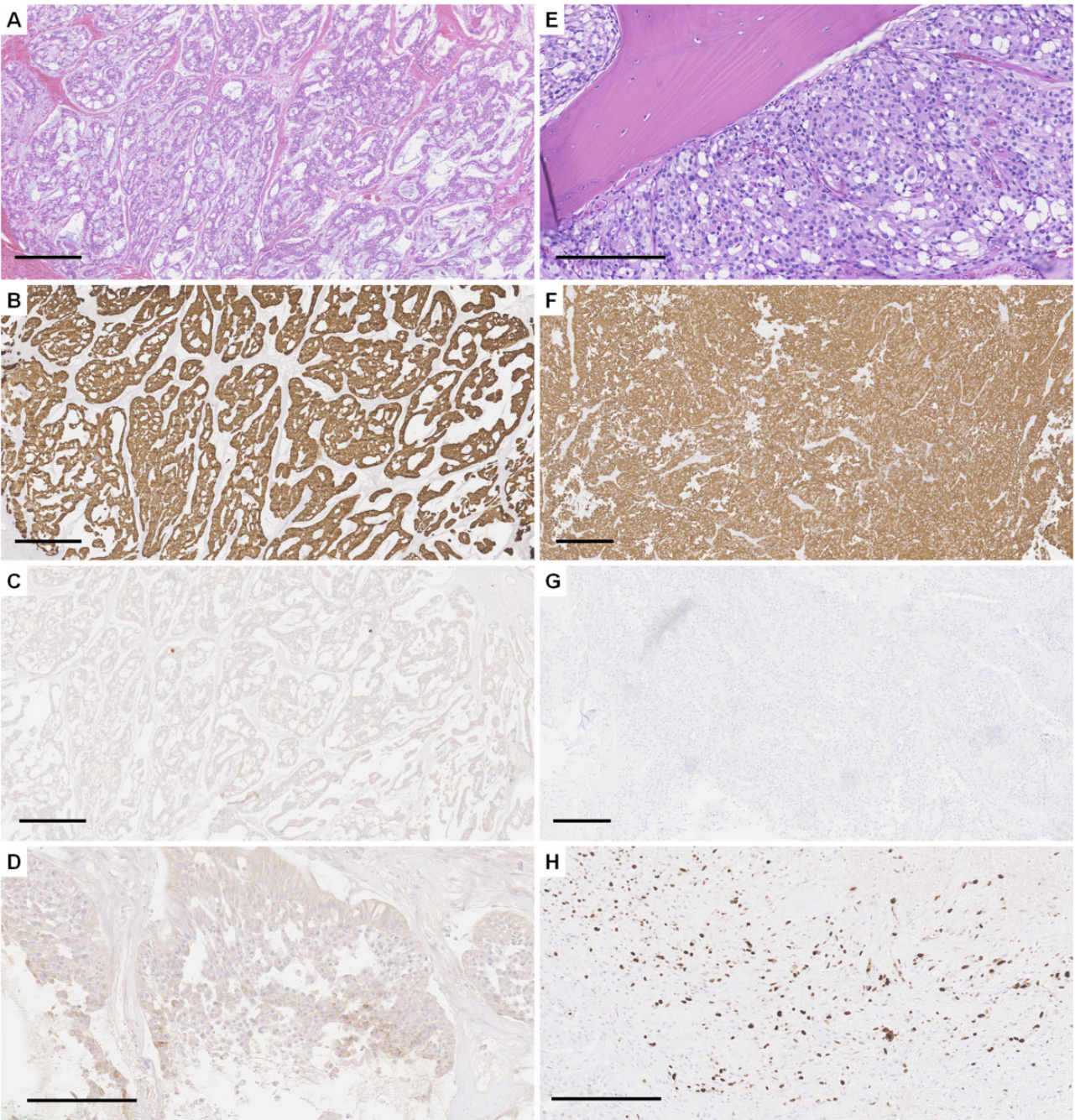


FIGURE 3. Microscopic sections from the initial resection of Case 2, demonstrating papillary and cribriform architecture with focal features suggestive of myxopapillary ependymoma (**A**). There was strong and diffuse positivity for GFAP (**B**), no immunoreactivity for CAM5.2 (**C**), and focal, dot-like staining for EMA (**D**), as well as microscopic sections from a recurrent specimen showing atypical features and invasion into bone (**E**), strong and diffuse reactivity for GFAP (**F**), no staining for CAM5.2 (**G**), and an increased Ki-67 proliferation index (**H**). **A–C**: magnifications, 50 \times , scale bars = 500 μ m; **D, F, G**: magnifications, 200 \times , scale bars = 200 μ m; **E, H**: magnifications, 100 \times , scale bars = 200 μ m.

DISCUSSION

MPE with anaplastic features are exceptionally rare with >20 confirmed cases described in the literature (Table 1) (21–26), and without distinctly defined pathologic features or established grade as of the most recent edition of the WHO

Classification of Tumours of the Central Nervous System (4). The potential malignant behavior of MPEs was firstly hypothesized by Davis and Barnard in 1985 (39). The authors reported 3 cases of MPE of the lumbar region with intracranial metastasis without clear identification of anaplastic features,

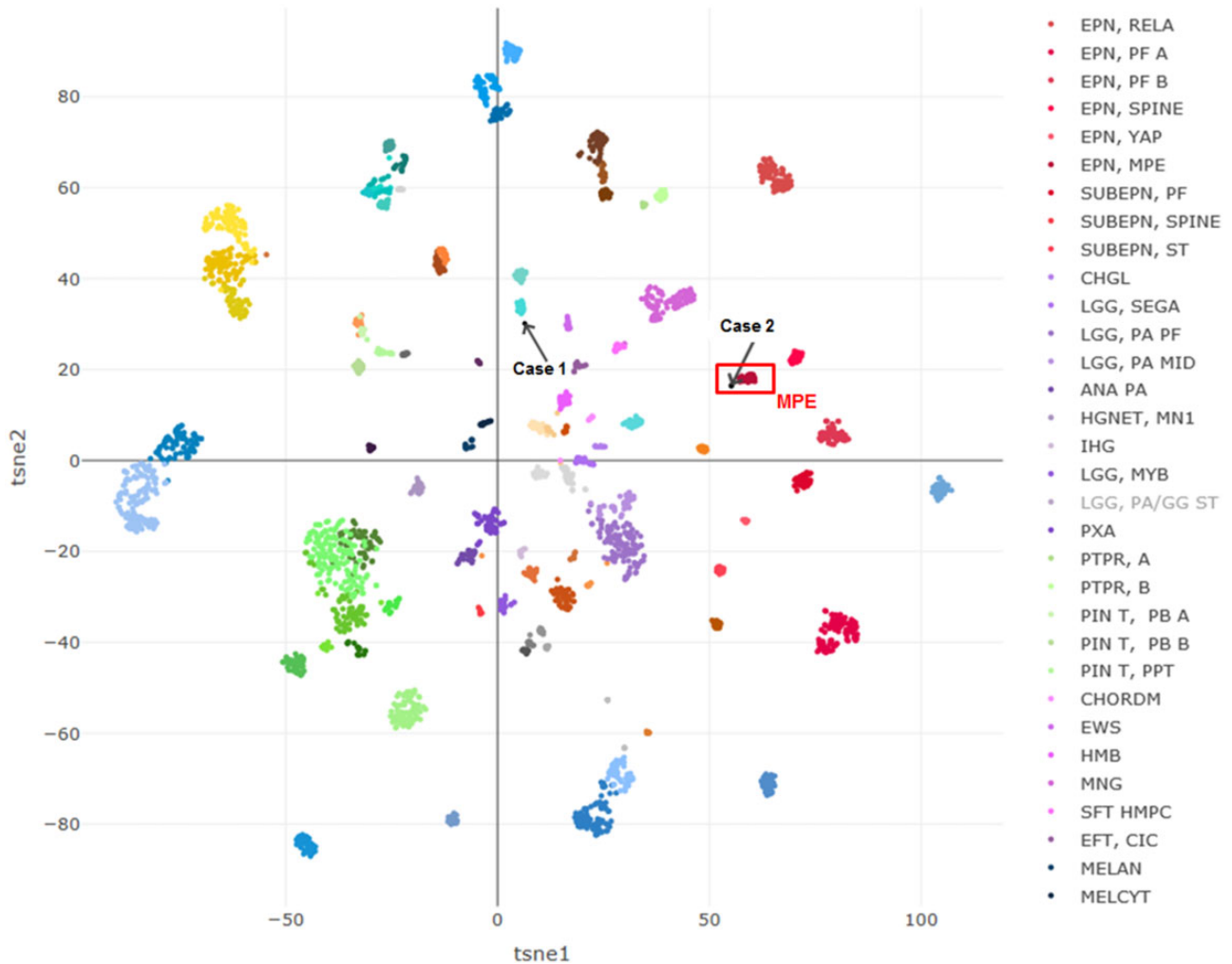


FIGURE 4. t-Distributed Stochastic Neighbor Embedding (t-SNE) plot showing the clustering of Cases 1 and 2 in relation to reference methylation groups for other tumor classes.

which has subsequently been shown in numerous cases, especially those with extradural components (11–16, 19, 20). All the patients underwent radiotherapy with delayed recurrence of the tumor. Since then, other cases of MPE showing possible anaplastic features have been reported in the literature; since no consensus criteria for anaplasia has been established the “anaplastic features” noted in these previous reports tend to be features that are extremely uncommon in the majority of MPE cases, as well as being features commonly associated with anaplasia in other tumor groups including conventional ependymomas, oligodendrogliomas, and astrocytomas (4, 40). Previously described cases of anaplastic MPE tend to have significantly worse clinical courses with higher morbidity, more frequent recurrences, and may have a higher rate of metastasis than their histologically benign counterparts. These tumors have loss of papillary architecture/focal solid areas and more significant atypical nuclear features (although atypia can also be found in conventional MPE), as well as higher mitotic counts (>5/10 HPF), higher Ki-67 indices (>10% and as high as 80% compared with <2% for conventional MPE), and fre-

quent necrosis and microvascular proliferation (Table 1). It is notable, however, that even benign-appearing MPEs may metastasize to other portions of the CNS or lymph nodes (especially in extradural cases), perhaps in part due to increased lymphatic proximity when these tumors grow beyond the spinal cord (26, 39, 41).

In our study, both MPE arose from the lumbosacral spine: One case presented as a classic benign MPE and the other had atypical features at initial presentation, but there was early recurrence of the tumors in both cases (12 and 14 months) after surgical excision and radiotherapy, as well as other aggressive features including invasion into bone and lymph node metastasis. Similar to previous cases in the literature, the cases represented in this report had significantly different ages (21 vs 72 years), but both presented as large tumors with high proliferation rates, microvascular proliferation, and necrosis (Table 2). Notably, the 2 cases in this report appear to represent the 2 largest MPEs with anaplasia described thus far (Table 1). In this study, immunohistochemical stains showed positivity for GFAP and S-100 in both cases,

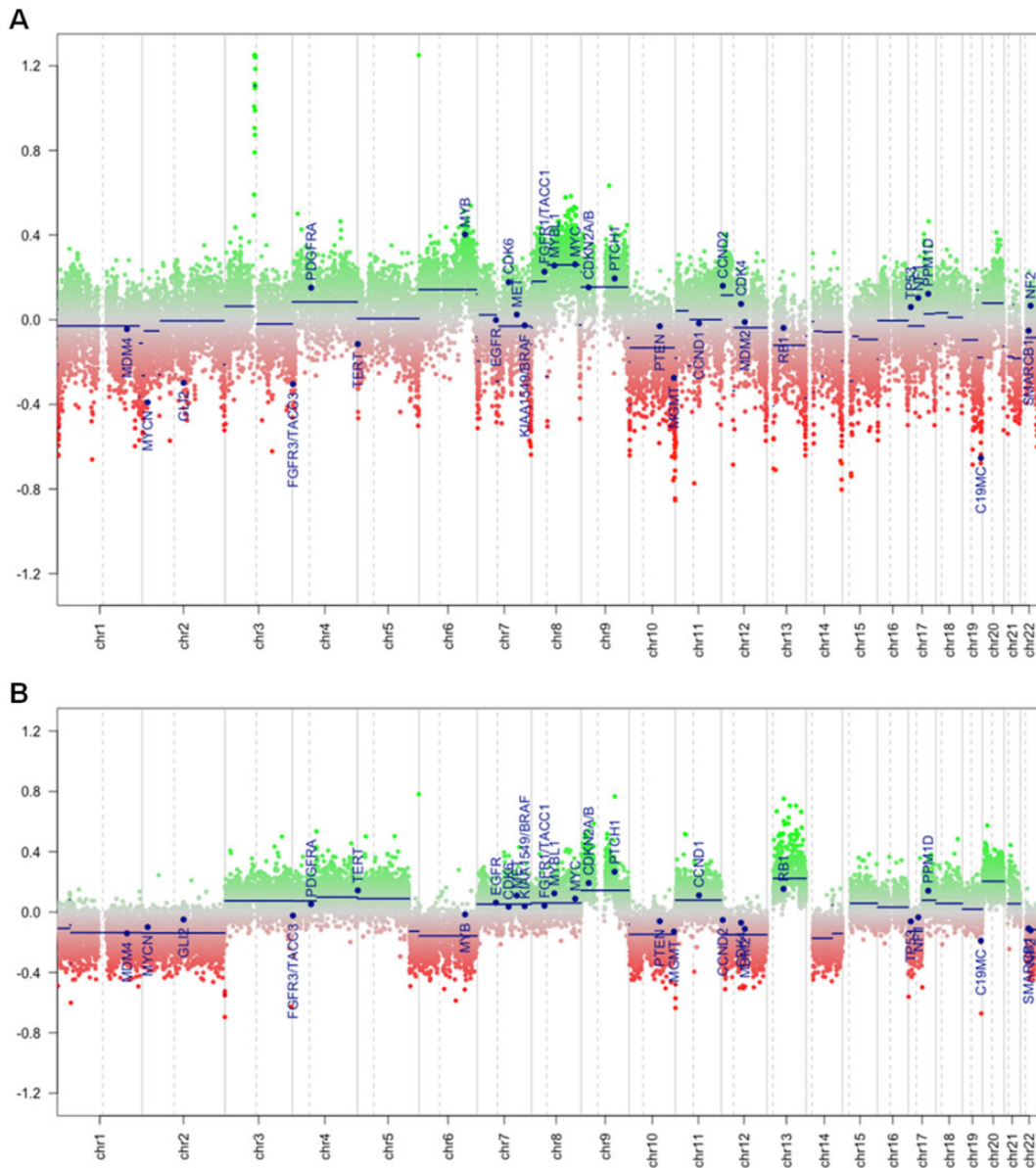


FIGURE 5. Copy number plots for Case 1 (A) and Case 2 (B).

confirming the typical immunophenotype patterns of MPEs. CAM5.2 was focally positive in Case 1 in the high-grade-appearing areas. EMA was negative in Case 1 in both primary and recurrent tumors; however, in Case 2, EMA staining was positive in the primary tumor before excision but negative in the recurrence. This could be explained by the anaplastic transformation with loss of the typical ependymal cell differentiation.

Characterization of molecular features has recently been of increasing relevance in the diagnosis and prognosis of various groups of ependymomas (5, 37). Among other abnormalities, supratentorial ependymomas have been demonstrated to frequently have *RELA* fusion genes as oncogenic drivers (5, 42, 43), spinal ependymomas have been shown to

frequently harbor chromosome 22q alterations, which includes the *NF2* locus (5, 37, 44, 45), and spinal subependymomas frequently harbor deletions in chromosome 6q (5). Spinal MPEs tend to exhibit aneuploidy or hyperdiploidy across multiple chromosomes, and this appears to be the case in anaplastic MPEs as well (5, 26, 37, 40), but no genes associated with MPE development, recurrence, or progression to anaplasia have yet been definitively established. Some studies suggest *EGFR* expression may be associated with MPE recurrence (46), although this has been disputed by other reports (47). Methylation profiling has also helped to group ependymomas of various histologic classifications and grades and locations into separate categories based on epigenetic features (Supplementary Data Table S1) (5), and

TABLE 2. Summary of Clinical and Pathologic Features in Cases 1 and 2

Case	Sex, Age	Pathology					Radiation Therapy	Recurrence (Time After Surgical Excision)	Metastasis	Survival	
		Location	Size	Necrosis	Microvascular Proliferation	Ki-67					Mitotic Figures
1	M, 72 y	Sacrum	13.0 × 4.3 × 2.3 cm	Yes	Yes	>50%	8/10 HPF	Yes	12 months	No	No
2	M, 21 y	Sacrum	13.3 × 9.3 × 8.2 cm	Yes	Yes	>10%	4/10 HPF	Yes	14 months	Regional lymph nodes	Yes

this has resulted in new prognostic categories among some of these subgroups.

The molecular analysis performed on the recurrent specimens from both cases demonstrates similar aneuploidy as previously identified in MPEs with anaplastic features with frequent partial and whole chromosome gains and losses (Fig. 5), while our targeted NGS panel similarly found no definitive mutational driver in either case. A unique aspect of this report is that it includes the first methylation profiling of anaplastic MPEs, although we did not identify grouping of our 2 cases on t-SNE. We demonstrate that while Case 2 is not an exact match for the MPE methylation cluster by t-SNE, this tumor does cluster relatively closely to the MPE group and away from spinal ependymoma, subependymoma, and posterior fossa ependymoma subgroups (Fig. 4).

In conclusion, anaplastic transformation of MPE is an extremely rare event, but it should be considered in the differential diagnosis of spinal tumors, especially in patients with a filum terminale or lumbosacral tumor or history of MPE and a clinically aggressively-behaving tumor in this location. As no definitive histopathological classification is available, the diagnosis of this entity is often difficult to establish and there is a need to determine specific microscopic or molecular criteria. Additionally, with only 19 cases available for review in the literature, the clinical implications of anaplastic features remain uncertain. As importantly, extradural and extraspinal MPEs have a significantly increased risk of aggressive behavior, even without histologic features suggestive of anaplasia, and thus tumors in this location should not automatically be treated as clinically benign (11–20).

The pathologist must be aware of the most common microscopic and immunohistochemical features of this rare tumor to avoid misinterpretation that can lead to incorrect treatment. Moreover, molecular studies should be considered as a part of the thorough pathological investigation since they can give useful information to identify and understand patterns of gene and chromosome abnormalities underpinning the tumor growth, proliferation, and transformation in such cases. While many conventional MPEs have been shown to have a hyperdiploid genome, work remains to be done to establish the specific drivers of MPE as well as genes and chromosomal regions which may increase the risk of anaplastic transformation or otherwise aggressive clinical behavior. Since MPE with anaplastic features shows aggressive behavior and an increased propensity for recurrence, it must be taken into account in the clinical practice to grant proper management of the patient.

REFERENCES

- Ostrom QT, Gittleman H, Truitt G, et al. CBTRUS statistical report: Primary brain and other central nervous system tumors diagnosed in the United States in 2011–2015. *Neuro Oncol* 2018;20:iv1–iv86
- Khalid SI, Kelly R, Adogwa O, et al. Pediatric spinal ependymomas: An epidemiologic study. *World Neurosurg* 2018;115:e119–e28
- Khalid SI, Adogwa O, Kelly R, et al. Adult spinal ependymomas: An epidemiologic study. *World Neurosurg* 2018;111:e53–e61
- WHO Classification of Tumours of the Central Nervous System. Revised 4th ed. Lyon, France: International Agency for Research on Cancer (IARC) 2016
- Pajtler KW, Witt H, Sill M, et al. Molecular classification of ependymal tumors across all CNS compartments, histopathological grades, and age groups. *Cancer Cell* 2015;27:728–43
- Kernohan JW. Primary tumors of the spinal cord and intradural filum terminale. In: Penfield W, ed. *Cytology & Cellular Pathology of the Nervous System*. New York, NY: P.B. Hoeber, Inc. 1932:993–1025
- Ilhan A, Furtner J, Birner P, et al. Myxopapillary ependymoma with pleuropulmonary metastases and high plasma glial fibrillary acidic protein levels. *J Clin Oncol* 2011;29:e756
- Kraetzig T, McLaughlin L, Bilsky MH, et al. Metastases of spinal myxopapillary ependymoma: Unique characteristics and clinical management. *J Neurosurg Spine* 2018;28:201–8
- Fonseca L, Cicuendez M, Martinez-Ricarte F, et al. A rare case of an intramedullary metastasis of a myxopapillary ependymoma. *Surg Neurol Int* 2019;10:83
- Akyurek S, Chang EL, Yu TK, et al. Spinal myxopapillary ependymoma outcomes in patients treated with surgery and radiotherapy at M.D. Anderson Cancer Center. *J Neurooncol* 2006;80:177–83
- Kline MJ, Kays DW, Rojiani AM. Extradural myxopapillary ependymoma: Report of two cases and review of the literature. *Pediatr Pathol Lab Med* 1996;16:813–22
- Fourney DR, Fuller GN, Gokaslan ZL. Intraspinial extradural myxopapillary ependymoma of the sacrum arising from the filum terminale externa. Case report. *J Neurosurg* 2000;93:322–6
- Vagaiwala MR, Robinson JS, Galicich JH, et al. Metastasizing extradural ependymoma of the sacrococcygeal region: Case report and review of literature. *Cancer* 1979;44:326–33
- Fassett DR, Schmidt MH. Lumbosacral ependymomas: A review of the management of intradural and extradural tumors. *Neurosurg Focus* 2003; 15:1–5
- Quraishi NA, Wolinsky JP, Bydon A, et al. Giant destructive myxopapillary ependymomas of the sacrum. *J Neurosurg Spine* 2010;12:154–9
- Batich KA, Riedel RF, Kirkpatrick JP, et al. Recurrent extradural myxopapillary ependymoma with oligometastatic spread. *Front Oncol* 2019;9: 1322
- Hendren TH, Hardin CA. Extradural metastatic ependymoma. *Surgery* 1963;54:880–2
- Morantz RA, Kepes JJ, Batnitzky S, et al. Extraspinal ependymomas. Report of three cases. *J Neurosurg* 1979;51:383–91
- Sonneland PR, Scheithauer BW, Onofrio BM. Myxopapillary ependymoma. A clinicopathologic and immunocytochemical study of 77 cases. *Cancer* 1985;56:883–93
- Schiavello E, Biassoni V, Antonelli M, et al. Pediatric extraspinal sacrococcygeal ependymoma (ESE): An Italian AIEOP experience of six cases and literature review. *Childs Nerv Syst* 2018;34:1291–8

21. Awaya H, Kaneko M, Amatyia VJ, et al. Myxopapillary ependymoma with anaplastic features. *Pathol Int* 2003;53:700–3
22. Beschoner R, Wehrmann M, Ernemann U, et al. Extradural ependymal tumor with myxopapillary and ependymoblastic differentiation in a case of Schinzel-Giedion syndrome. *Acta Neuropathol* 2007;113:339–46
23. Chakraborti S, Kini H, Pai KG, et al. Sacrococcygeal myxopapillary ependymoma with anaplastic ependymoma component in an infant. *J Pediatr Neurosci* 2012;7:218–20
24. Trivedi D, Xiong Z. Anaplastic myxopapillary ependymoma in an infant: Case report and literature review. *Intract Rare Dis Res* 2017;6:128–31
25. Huynh TR, Lu C, Drazin D, et al. Myxopapillary ependymoma with anaplastic features: A case report with review of the literature. *Surg Neurol Int* 2018;9:191
26. Lee JC, Sharifai N, Dahiya S, et al. Clinicopathologic features of anaplastic myxopapillary ependymomas. *Brain Pathol* 2019;29:75–84
27. Serrano J, Snuderl M. Whole genome DNA methylation analysis of human glioblastoma using illumina BeadArrays. *Methods Mol Biol* 2018;1741:31–51
28. Capper D, Jones DTW, Sill M, et al. DNA methylation-based classification of central nervous system tumours. *Nature* 2018;555:469–74
29. Sturm D, Witt H, Hovestadt V, et al. Hotspot mutations in H3F3A and IDH1 define distinct epigenetic and biological subgroups of glioblastoma. *Cancer Cell* 2012;22:425–37
30. Wiestler B, Capper D, Hovestadt V, et al. Assessing CpG island methylator phenotype, 1p/19q codeletion, and MGMT promoter methylation from epigenome-wide data in the biomarker cohort of the NOA-04 trial. *Neuro Oncol* 2014;16:1630–8
31. Wiestler B, Capper D, Sill M, et al. Integrated DNA methylation and copy-number profiling identify three clinically and biologically relevant groups of anaplastic glioma. *Acta Neuropathol* 2014;128:561–71
32. Orillac C, Thomas C, Dastagirzada Y, et al. Pilocytic astrocytoma and glioneuronal tumor with histone H3 K27M mutation. *Acta Neuropathol Commun* 2016;4:84
33. Huse JT, Snuderl M, Jones DT, et al. Polymorphous low-grade neuroepithelial tumor of the young (PLNTY): An epileptogenic neoplasm with oligodendroglioma-like components, aberrant CD34 expression, and genetic alterations involving the MAP kinase pathway. *Acta Neuropathol* 2017;133:417–29
34. Richardson TE, Snuderl M, Serrano J, et al. Rapid progression to glioblastoma in a subset of IDH-mutated astrocytomas: A genome-wide analysis. *J Neurooncol* 2017;133:183–92
35. Richardson TE, Patel S, Serrano J, et al. Genome-wide analysis of glioblastoma patients with unexpectedly long survival. *J Neuropathol Exp Neurol* 2019;78:501–7
36. Richardson TE, Tang K, Vasudevaraja V, et al. GOPC-ROS1 fusion due to microdeletion at 6q22 is an oncogenic driver in a subset of pediatric gliomas and glioneuronal tumors. *J Neuropathol Exp Neurol* 2019;78:1089–99
37. Hirose Y, Aldape K, Bollen A, et al. Chromosomal abnormalities subdivide ependymal tumors into clinically relevant groups. *Am J Pathol* 2001;158:1137–43
38. Mack SC, Agnihotri S, Bertrand KC, et al. Spinal myxopapillary ependymomas demonstrate a Warburg phenotype. *Clin Cancer Res* 2015;21:3750–8
39. Davis C, Barnard RO. Malignant behavior of myxopapillary ependymoma. Report of three cases. *J Neurosurg* 1985;62:925–9
40. Prayson RA. Myxopapillary ependymomas: A clinicopathologic study of 14 cases including MIB-1 and p53 immunoreactivity. *Mod Pathol* 1997;10:304–10
41. Ma YT, Ramachandra P, Spooner D. Case report: Primary subcutaneous sacrococcygeal ependymoma: A case report and review of the literature. *Br J Radiol* 2006;79:445–7
42. Pietsch T, Wohlers I, Goschzik T, et al. Supratentorial ependymomas of childhood carry C11orf95-RELA fusions leading to pathological activation of the NF-kappaB signaling pathway. *Acta Neuropathol* 2014;127:609–11
43. Parker M, Mohankumar KM, Punchihewa C, et al. C11orf95-RELA fusions drive oncogenic NF-kappaB signalling in ependymoma. *Nature* 2014;506:451–5
44. Ebert C, von Haken M, Meyer-Puttlitz B, et al. Molecular genetic analysis of ependymal tumors. NF2 mutations and chromosome 22q loss occur preferentially in intramedullary spinal ependymomas. *Am J Pathol* 1999;155:627–32
45. Yokota T, Tachizawa T, Fukino K, et al. A family with spinal anaplastic ependymoma: Evidence of loss of chromosome 22q in tumor. *J Hum Genet* 2003;48:598–602
46. Verma A, Zhou H, Chin S, et al. EGFR as a predictor of relapse in myxopapillary ependymoma. *Pediatr Blood Cancer* 2012;59:746–8
47. Wang H, Zhang S, Rehman SK, et al. Clinicopathological features of myxopapillary ependymoma. *J Clin Neurosci* 2014;21:569–73